

Analysis of the trace elements in micro-alloy steel by reheating double-pulse laser-induced breakdown spectroscopy

Jingge Wang¹ · Xinzhong Li¹ · Hehe Li¹ · Chuanlei Yin¹

Received: 22 August 2016 / Accepted: 29 March 2017 / Published online: 6 April 2017
© Springer-Verlag Berlin Heidelberg 2017

Abstract Two Q-switched Nd:YAG lasers at 1064-nm wavelength have been employed to detect the trace elements in microalloy steel samples by single-pulse and reheating double-pulse laser-induced breakdown spectroscopy. It is found that the emission lines intensities of the trace elements were significantly enhanced by reheating double-pulse scheme. Furthermore, the extent of the enhancement of the line intensity was related to the excitation energy level of the emission line. Then, the emission enhancement was explained by the investigation of the spatial resolution of the plasma temperatures. The results have shown that the enhancement mechanism can be attributed to the greater and hotter plasma generated by the re-excitation of the reheating laser pulse in double-pulse scheme. Finally, calibration plots were constructed for Mn, Cr, and Cu using a set of certified microalloy steel samples. The detection limits of the trace elements were calculated for the reheating double-pulse scheme and compared to those of single-pulse scheme. It has been shown that the detection limits of the trace elements were improved by a factor of 1.81–3.46 when the reheating double-pulse scheme was used.

1 Introduction

Laser-induced breakdown spectroscopy (LIBS) has become a powerful method for the analysis of the elemental composition of materials. It has been widely applied in a large

variety of fields [1–5] as a fast, simple, and multi-elemental detecting technique with capability of remote detection and spatial resolution. However, this technique suffers from a relatively low detection sensitivity compared to other traditional techniques. To overcome this problem, one of the most attractive approaches to improve the LIBS sensitivity is the double-pulse excitation scheme.

The double-pulse technique has initially been introduced by Cremers et al. [6]. It has demonstrated that the emission intensity can be enhanced significantly by double-pulse experiments. So far, several double-pulse configurations have been studied, differing on the geometrical configuration, the wavelength and the temporal order of the two laser beams. Mainly, the so-called collinear or orthogonal configuration was often used. In collinear geometry, both the laser pulses propagate along the same axis, perpendicularly to the target surface with certain interpulse time [7–9]. In the orthogonal geometry, two configurations have been proposed: the reheating scheme and the pre-ablation scheme. In the reheating scheme, the second pulse parallel to the target surface reheated the plasma induced by the first laser pulse [10, 11]. In the pre-ablation scheme, a pre-pulse spark was created in air before the ablation of the sample by the second pulse [12–14].

To obtain more insight into the double-pulse scheme, many efforts have been devoted to investigate the signal enhancement mechanism of the double pulse. As far as we are aware, there exist several explanations, such as an increased laser–plasma coupling [15], an increased sample heating [16], yielding more ablation [17], and ambient gas rarefaction [18]. One should keep in mind that the enhancement mechanism is different with the double-pulse configuration and interpulse time.

The benefits of improving detection limits by double-pulse scheme have also been reported in several researches.

✉ Jingge Wang
wangjingge1987@126.com

¹ School of Physics and Engineering, Henan University of Science and Technology, Luoyang 471023, China

Burakov et al. [19] investigated the application of the collinear double-pulse scheme for detecting heavy and toxic metals in soil samples. The detection limit for lead was improved to 20 ppm by double-pulse scheme. Ismail et al. [20] compared the limits of detection for several elements in aluminum and steel alloys, by use of the single and collinear double-pulse configurations. Detection limits were significantly improved by a factor of 1.5–10 for the elements by use of the double-pulse configuration.

It should be noted that, for spectroscopic measurements, most papers on the analytical performance of double-pulse LIBS mainly reported the use of the collinear double-pulse scheme because of its simple optical alignment. However, in the present study, we decided to fully evaluate the potentialities of the reheating orthogonal double-pulse approach. The aim of this study was to compare the reheating double-pulse scheme and the single pulse in detecting the trace elements of microalloy steels. For this purpose, the emission enhancements of the trace elements were investigated first. To better understand the enhancement mechanism, we then compare the spatial distribution of plasma temperatures of the reheating double-pulse scheme to that of the single-pulse scheme. The main ideas of enhancement mechanisms for the reheating double-pulse scheme will be discussed in this study. Finally, the results of the quantitative analysis for the trace elements were investigated for both schemes, and the improvements of the detection limits in the reheating orthogonal double-pulse scheme were determined.

2 Experimental setup

A schematic diagram of the experimental setup for a reheating orthogonal double-pulse configuration is shown in Fig. 1. A Q-switched Nd:YAG laser (Quantel laser company) operating at the fundamental wavelength of 1064 nm was used as the ablation laser. The pulse energy was 45 mJ,

and the pulse duration was 8 ns. The laser beam was aligned perpendicular to the sample surface and focused by a plano-convex lens with a 100-mm focal length. The second laser used for reheating the plasma was also a Q-switched Nd:YAG laser with the same parameters as the ablation laser. The beam of the second laser was directed parallel to the sample surface and perpendicular to the ablation laser beam. A lens of 90-mm focal length ensured the focusing of the second laser beam in the plasma induced by the first laser. A delay generator (SRS, DG645) controlled the delay time between the two laser pulses. The measurements were carried out in air at atmospheric pressure. The second laser pulse hit the microplasma at a height of about 1.5 mm above the sample surface. This was the result of optimizing measurements showing that the emission intensity was just observed with increasing the distance between the focus position of the second laser pulse and the sample surface. It was proven experimentally that the second plasma had no measurable impact on the surface of the sample. When comparing double-pulse effects, the zero delay time between the two lasers was used for comparison. The total pulse energy was 80 mJ for both single pulse (two lasers with zero delay time) and double pulses. For double-pulse configuration, the interpulse delay was set to 200 ns, which has been confirmed to be the optimal delay time for reheating double pulse in our previous study [21].

For quantitative analysis, an UV–NIR light collector (Andor technology) was used to couple the whole plasma emission into the fiber (Fig. 1a). On the other hand, in order to analyze the enhancement mechanism of reheating double-pulse scheme, the spatial resolved spectra were acquired by an optical system consisting of two lenses with focal length of 10 mm (Fig. 1b). This system allowed us to detect the local region of the plasma on the image plane, as shown in Fig. 1c. The core diameter of the optical fiber was 0.1 mm. The plasma emission was sent to an Echelle spectrometer (Andor technology, Mechelle 5000) equipped

Fig. 1 Schematic diagram of the experimental system. **a** Collecting system for the whole plasma, **b** collecting system for spatial distributions of the plasma, and **c** scheme of the points of the plasma for measurement

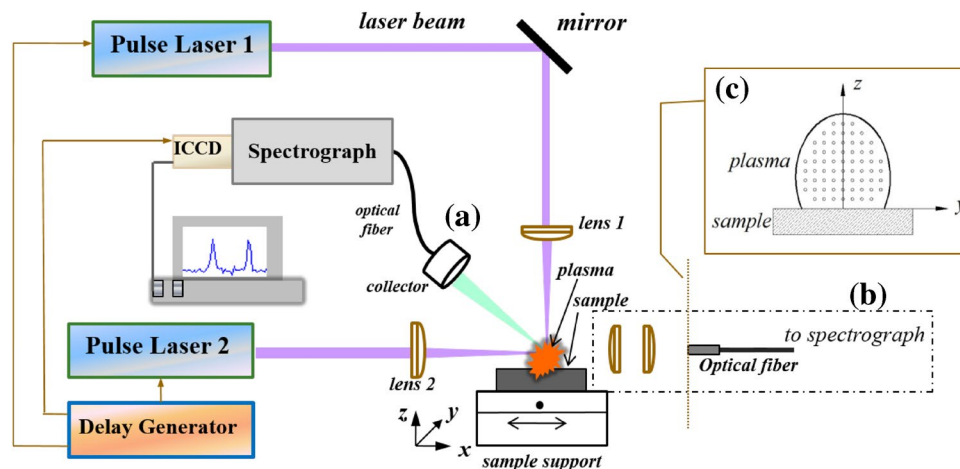


Table 1 Certified concentrations of Mn, Cr, and Cu in the microalloy steel samples

Sample	Mn (wt%)	Cr (wt%)	Cu (wt%)
1#	0.151	0.164	0.154
2#	1.1	0.322	0.201
3#	0.571	0.092	0.105
4#	1.50	0.409	0.054
5#	2.00	0.601	0.021
6#	0.110	0.062	0.288
7#	0.043	0.036	0.346

with an intensified charge-coupled device (ICCD) detector (Andor technology, iStar 734). The ensemble provided a spectral range from 230 to 920 nm, a resolution power ($\lambda/\Delta\lambda$) of 5000. The ICCD was triggered by the Q-switch of the second laser. A gate width of 10 μs preceded by a delay of 1 μs was used for spectral detection in quantitative measurements. While, for spatial resolved spectra, the gate delay and width were both set to 1 μs .

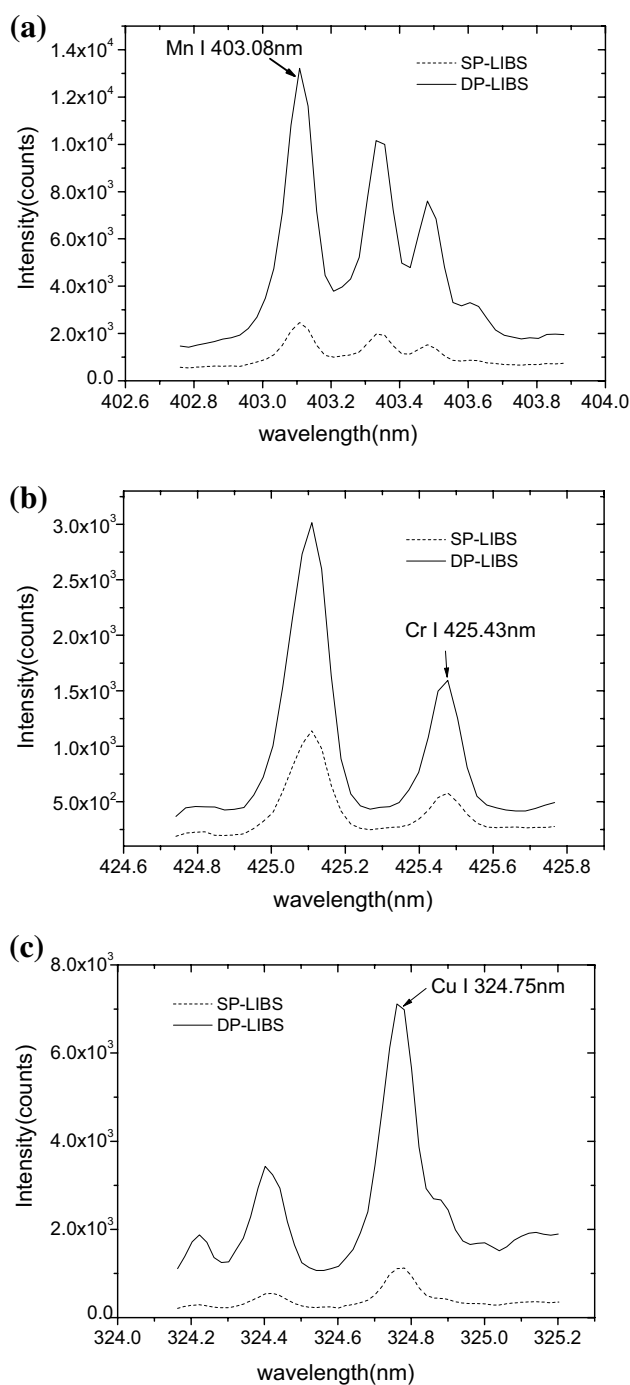
A set of microalloy steel certified samples (NCS Testing Technology Co., Ltd) were used for quantitative analysis. In our study, trace elements including Mn, Cr, and Cu were selected for detection. Table 1 lists the certified concentrations of these three elements in seven microalloy steel samples.

The repetition frequency of the two lasers was both set to 1 Hz. For each new measurement, before spectral collection, 20 laser pulses were performed to clean the sample surface and remove surface oxides and contamination to ensure that the observed spectrum is representative of the sample composition. Samples presented for analysis are located on a fast translation stage that moves the sample between laser pulses, thereby exposing a fresh region of the sample to each successive laser pulse. For spatial resolved spectra, each spectrum was accumulated for 20 laser pulses. However, in order to reduce the influence of signal fluctuations, each spectrum was accumulated for 50 laser pulses for quantitative analysis. Ten spectra were acquired for each sample listed in Table 1, to evaluate the standard deviation of the measurement.

3 Results and discussion

3.1 Enhancement of spectral line intensity

The strongest spectral lines of the trace elements were selected for analysis. For Mn, Cr, and Cu, the analyzed line is Mn I @ 403.08 nm, Cr I @ 425.43 nm, and Cu I @ 324.75 nm, respectively. Figure 2 shows the characteristics of the spectral line intensity detected by single-pulse

**Fig. 2** Emission spectra of the trace elements produced by single-pulse scheme (SP-LIBS) and reheating double-pulse scheme (DP-LIBS)

and reheating double-pulse configurations. It is clear that the emission intensity was enhanced in double-pulse experiments. Specifically, the reheating pulse lead to an enhancement of about a factor 5 for Mn I @ 403.08 nm, 3 for Cr I @ 425.43 nm, and 6 for Cu I @ 324.75 nm. One can conclude that the reheating double-pulse scheme

is more sensitive to detect the trace elements in microalloy steel. Moreover, it can be seen that Cu I @ 324.75 nm (with excitation energy level of 3.82 eV) and Mn I @ 403.08 nm (with excitation energy level of 3.08 eV) have a better enhancement than that of Cr I @ 425.43 nm (with excitation energy level of 2.91 eV). The different enhancements could be related to the excitation energy levels of the line emissions. It has been validated by Gautier et al. [22, 23] that the line emissions with the higher excitation energy levels have the greater enhancements in reheating double-pulse arrangements. The emission signal enhancement mechanism in reheating double-pulse scheme will be explained in the next section by analyzing the plasma temperature.

3.2 Emission enhancement mechanism

The emission enhancement mechanism of double-pulse LIBS in different configurations have been investigated in several researches. In the reheating orthogonal double-pulse scheme, the major reason for enhancement is the re-excitation mechanisms by the second laser pulse to the plasma ablated by the first laser pulse. In a previous paper of our study, by time-resolved fast-photography of the plasma, it has been shown that the height and width of the plasma were increased in the reheating double-pulse scheme [24]. In the present study, to understand the signal performed in the double-pulse and single-pulse schemes, the combining optical system formed the image of the plasma onto the plane of one end of the optical fiber. The core diameter of the optical fiber was 0.1 mm. The fiber was fixed on a translation stage with micrometer precision, and it can be displaced in steps of 0.1 mm along the lateral (y) and axial (z) directions. It should be emphasized that the spectra at a given lateral position (as in Fig. 1c) of the plasma are integrated along the line-of-sight on the x axis. If these spectra were used to determine the parameters of the plasma temperature, then the values are the population average along the line-of-sight.

Assuming the local thermodynamics equilibrium (LTE), the Boltzmann plot method [25] was applied to determine plasma temperatures. In the current study, 11 Fe I spectral lines detected simultaneously by the Echelle spectrometer were selected to perform Boltzmann plots. The parameters of the transitions were taken from the NIST Atomic Spectra Database [26], and are indicated in Table 2. In Fig. 3, we show typical examples of the Boltzmann plots on the axis of the plasma in the single- and double-pulse experiments.

The emission intensity is too weak to be measurable at some positions at the front and interior of the plasma. Therefore, only the plasma temperatures of a region of the plasma with stronger intensity were obtained by the

Table 2 Spectroscopic constants of Fe I lines used in Boltzmann plot temperature determination

Wavelength/nm	E_i /eV	E_k /eV	A_{ki}/s^{-1}	g_k
344.06	0	3.60	1.71E+07	7
360.67	2.69	6.13	8.29E+07	13
361.88	0.99	4.42	7.22E+07	7
371.99	0	3.33	1.62E+07	11
374.55	0.09	3.40	1.15E+07	7
385.99	0	3.21	9.69E+06	9
396.93	1.49	4.61	2.26E+07	7
411.85	3.57	6.58	4.96E+07	13
423.59	2.43	5.35	1.88E+07	9
430.79	1.56	4.44	3.38E+07	9
440.48	1.56	4.37	2.75E+07	9

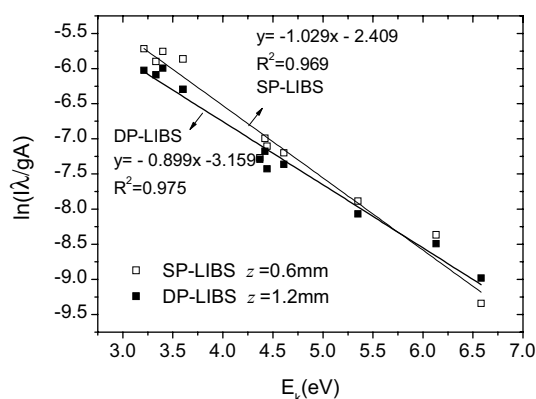


Fig. 3 Examples of Boltzmann plots in the SP-LIBS and DP-LIBS (gate width t_w : 1 μ s; gate delay time t_d : 1 μ s; SP-LIBS in thin line, and DP-LIBS in thick line). The slope of the Boltzmann plot is $(-1/\kappa_B T)$

Boltzmann plots. The spatial distributions of the plasma temperatures in single-pulse and double-pulse schemes were shown in Fig. 4. As seen in the figure, the plasma temperatures in double-pulse scheme are significantly higher than that of single-pulse scheme. The effective region in the plasma for Boltzmann plot temperature determination was also increased in double-pulse scheme. In single-pulse scheme, the plasma temperature has the maximum at the center position on the lateral direction (y) with an axial position (z) of 0.3 mm, and decreases for the increasing axial and transverse distances. However, in double-pulse scheme, the spatial evolution of the plasma temperature shows a more complex trend. As shown in Fig. 4b, the plasma temperature values at the border of the plasma were lower than that in the central regions. On the axial direction, moving away from the target, the plasma temperature increases first and reaches a maximum at a position

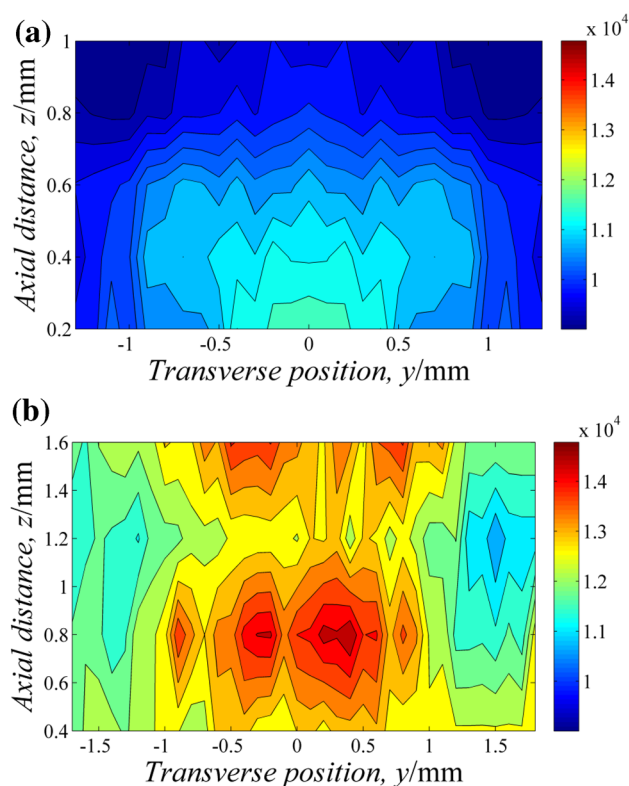


Fig. 4 Spatial distributions of the plasma temperature for single-pulse scheme (SP-LIBS) and reheating double-pulse scheme (DP-LIBS). **a** SP-LIBS, **b** DP-LIBS

of 0.8 mm, then decreases with the increasing distance. However, when the distance is greater than 1.3 mm, it is noticed that the plasma temperature values rises again until the front-head of the analyzing region. This observation is caused by the re-exciting mechanism by the second laser pulse. The position of the second hotter region in the plasma on the axis direction was corresponding to the focus position of the second laser pulse. Once the second laser energy is absorbed by the plasma ablated by the first laser pulse, the collision between the particles (electron, ions, and atoms) in the plasma plume become more stronger, which result in higher plasma temperature. On the other hand, more particles in the plasma were ablated during the laser–matter interaction, so the hotter region in the plasma was produced. Finally, the greater and hotter plasma in double-pulse scheme will result in the significant enhancement of the emission spectra. Meanwhile, in the reheating process by the second pulse, the population of upper states with high-lying excitation energies increases. Hence, the intensity enhancement is greater for the lines coming from higher excitation energy levels. As shown in Sect. 3.1 of this paper, the strongest enhancement was found for Cu I @ 324.75 nm.

3.3 Quantitative analysis

In the last two sections, it has been shown that the emission intensity is significantly increased by reheating double-pulse scheme. That is, the trace elements can be more sensitively detected by double-pulse mode. In the present section, we measured the concentrations of the trace elements (Mn, Cr, and Cu) in the microalloy steel as listed in Table 1 in double-pulse and single-pulse scheme.

Several ways have been proposed to obtain quantitative information of the samples from LIBS measurements. The internal standard method [27] is useful when the concentration of a major element present in all samples is either know or constant. In our studies, for steel samples, iron is considered as an element with constant concentration, which can be used as the best element for the internal standard. In this case, the calibration curves of the elements of interest can be obtained by drawing the relative intensities of the specific emission lines of these elements against their certified concentrations. Here, the relative intensities refer to the emission line intensities of the elements of interest (Mn, Cr, and Cu) normalized by the line intensities of the internal standard element (Fe). In actual measurements, one should be cautious in selecting the analysis and internal standard lines. The theoretical principles of internal standardization have been studied in Barnett's studies [28]. Firstly, the emission lines should be required to have minimal interference from other emission lines, and are intense enough with negligible self-absorption effect. Furthermore, the selection of internal standard line pairs requires the judicious balancing of the major temperature dependent factors, i.e., populations of excited states, degree of ionization, and partition function behavior. Taking into account these principles, for Mn, Cr, and Cu, the emission lines of Mn I @ 403.08 nm, Cr I @ 425.43 nm, and Cu I @ 324.75 nm are selected as the analyzed lines. Further, the corresponding internal standard lines are Fe I @ 373.71 nm, Fe I @ 385.99 nm, and Fe I @ 371.99 nm, respectively.

The calibration curves for the trace elements (Mn, Cr, and Cu) in single-pulse and double-pulse schemes are given in Fig. 5. Each data point represents the mean value of typically ten individual measurements. The given error bars show the calculated standard deviation for the measurements. As can be seen in Fig. 4, in double-pulse scheme, the calibration curves of the three elements have steeper slopes than that in single-pulse scheme. It has been known that the slope of the calibration curve represents the sensitivity of the measurement. The differences in the degree of improvement for different elements may depend on the element properties. Moreover, compared with single-pulse scheme, the correlation coefficients of the calibration

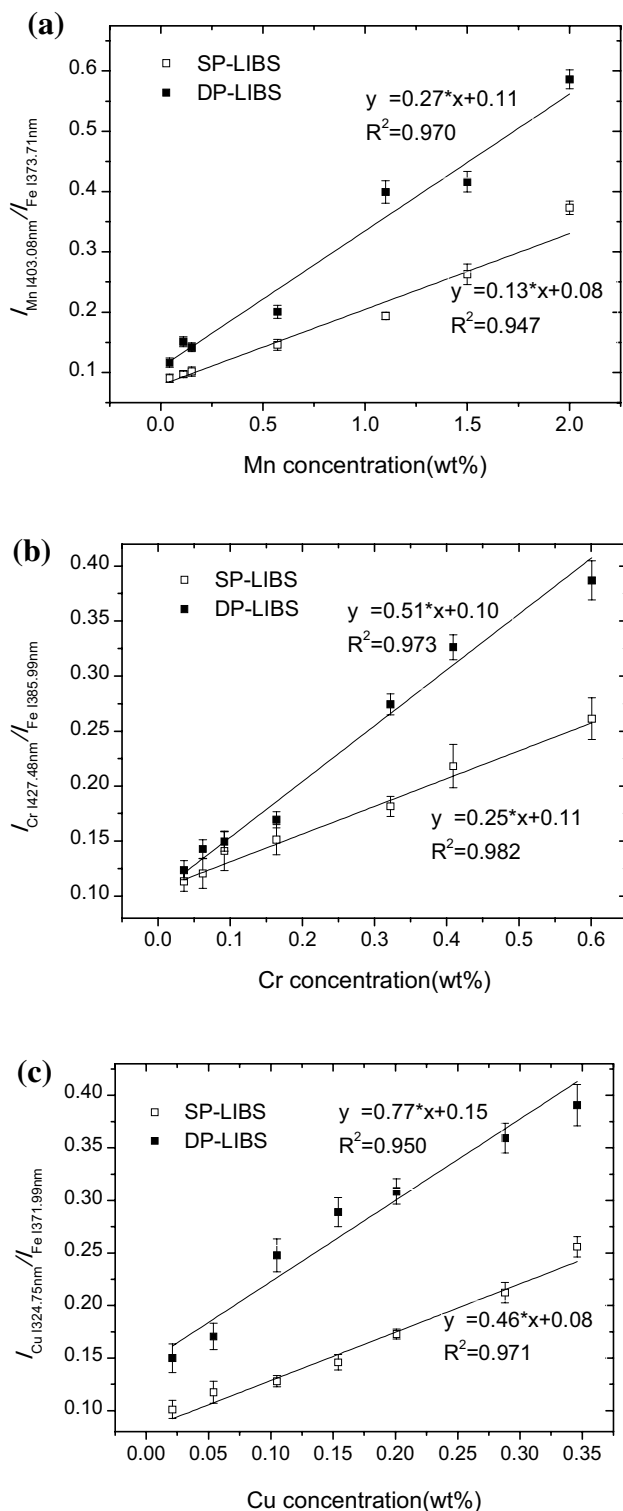


Fig. 5 Calibration plots obtained for manganese, chromium, and copper in microalloy steel by single-pulse and double-pulse schemes. Error bars represent the standard deviation of the intensity from ten replicate measurements

curves of Mn and Cr are slightly increased by double-pulse scheme. Thus, we can conclude that the detection sensitivity of the trace element in steel is improved by double-pulse scheme.

Detection limits were calculated according to the 3σ -IUPAC criterion [29] as follows:

$$\text{LOD} = 3 \frac{\sigma_B}{S}$$

where σ_B is the standard deviation of the continuum background nearby the analysis line of the specific element and S is the slope of the calibration curve of the corresponding element.

The detection limits for Mn, Cr, and Cu in the double-pulse experiments are compared to that of the single-pulse experiments in Table 3. One can see that the reheating double-pulse technique improves the limits of detection by a factor 1.81–3.46 for the trace elements in microalloy steels. It is obvious that the degrees of improvement are different for the three trace elements. In Sect. 3.1 of this paper, it has shown that the emission line intensity of Cu I @ 324.75 nm with higher excitation energy level has a better enhancement by double-pulse scheme. However, the extent of the improvement of detection limit was lowest for Cu. These observations may be explained in terms of background noise enhancement properties of different emission lines in the double-pulse configuration. As can be seen in Table 3, the analyzed line of Cu has the worst background noise properties both in the single-pulse and double-pulse configuration, which has a great influence on the detection of this element. However, further studies should be carried out to investigate this observation.

4 Conclusions

Two lasers operating at 1064 nm were set up in reheating orthogonal double-pulse geometry for the quantitative analysis of the trace elements in microalloy steel samples. General enhancement of the emission line intensity was observed for double-pulse spectra compared to single-pulse spectra. The emission line intensity of Cu I @ 324.75 nm has the best enhancement in double-pulse scheme. It is related to the high excitation energy of the emission line. The plasma temperature is a key parameter to understand the intensity enhancement mechanism of the reheating double-pulse scheme. The spatial resolution investigations of the plasma temperatures have shown that the significant enhancement of the emission spectra can be attributed to the greater and hotter plasma in reheating double-pulse

Table 3 Comparison of limits of detection obtained in the single- and double-pulse configurations for the trace elements in microalloy steel samples

Species	σ_B (SP) 10^{-3}	σ_B (DP) 10^{-3}	LOD (SP) 10^{-2} wt%	LOD (DP) 10^{-2} wt%	LOD (SP)/LOD (DP)
Cu	3.64	3.35	2.37	1.31	1.81
Cr	3.36	2.7	4.03	1.58	2.55
Mn	1.38	0.71	3.18	0.92	3.46

scheme. Comparing the quantitative analysis of the trace elements, it is found that the detection limits have been improved by the reheating double-pulse experiments.

Acknowledgements The authors are grateful for the financial support from National Natural Science Foundation of China (Grant No. 11504091).

References

- L. Peter, V. Sturm, R. Noll, *Appl. Opt.* **42**, 6199 (2003)
- P. Diwakar, P. Kulkarni, M.E. Birch, *Aerosol Sci. Technol.* **46**, 316 (2012)
- S. Morihisa, I. Akio, I. Chikara et al., *J. Nucl. Sci. Technol.* **51**, 930 (2014)
- J. Lasue, R.C. Wiens, S.M. Clegg et al., *J. Geophys. Res. Planets* **117**, E01001 (2012)
- A. De Giacomo, M. Dell'Aglio, O. De Pascale et al., *Spectrochim. Acta B* **63**, 585 (2008)
- D.A. Cremers, L.J. Radziemski, T.R. Loree, *Appl. Spectrosc.* **38**, 721 (1984)
- M. Corsi, G. Cristoforetti, M. Giuffrida et al., *Spectrochim. Acta B* **59**, 723 (2004)
- A.M. Matiaske, I.B. Gornushkin, U. Panne, *Anal. Bioanal. Chem.* **402**, 2597 (2012)
- G. Galaacs, N. Jedlinazki, K. Herrera et al., *Appl. Spectrosc.* **64**, 161 (2010)
- J. Uebbing, J. Brust, W. Sdorra et al., *Appl. Spectrosc.* **45**, 1419 (1991)
- V. Contreras, M.A. Meneses-Nava, O. Barbosa-Garcia et al., *Opt. Express* **37**, 4591 (2012)
- D.N. Stratis, K.L. Eland, S.M. Angel, *Appl. Spectrosc.* **54**, 1270 (2000)
- S.C. Choi, M.K. Oh, Y. Lee et al., *Spectrochim. Acta B* **64**, 427 (2009)
- J. Register, J. Scaffidi, S.M. Angel, *Appl. Spectrosc.* **66**, 869 (2012)
- A. Bogaerts, Z.Y. Chen, D. Autrique, *Spectrochim. Acta B* **63**, 746 (2008)
- R. Sanginés, H. Sobral, E. Alvarez-Zauco, *Spectrochim. Acta B* **68**, 40 (2012)
- A. Giacomo, M. Dell'Aglio, D. Bruno et al., *Spectrochim. Acta B* **63**, 805 (2008)
- G. Cristoforetti, S. Legnaioli, L. Pardini et al., *Spectrochim. Acta B* **61**, 340 (2006)
- V.S. Burakov, N.V. Tarasenko, M.I. Nedelko et al., *Spectrochim. Acta B* **64**, 141 (2009)
- M.A. Ismail, G. Cristoforetti, S. Legnaioli et al., *Anal. Bioanal. Chem.* **385**, 316 (2006)
- Q. Wang, F.Z. Dong, Y.X. Liang et al., *Acta Opt. Sin.* **31**, 1030002 (2011)
- C. Gautiera, P. Ficheta, D. Menuta et al., *Spectrochim. Acta B* **60**, 265 (2005)
- C. Gautiera, P. Ficheta, D. Menuta et al., *Spectrochim. Acta B* **59**, 975 (2004)
- J.G. Wang, H.B. Fu, Z.B. Ni et al., *Spectrosc. Spectr. Anal.* **36**, 817 (2016)
- S. Yalcin, D.R. Crosley, G.P. Smith et al., *Appl. Phys. B* **68**, 121 (1999)
- http://physics.nist.gov/PhysRefData/ASD/levels_form.html
- K. Barkonikos, L.N. Pasiadis, N.S. Thomaidis, *Talanta* **129**, 165 (2014)
- W.B. Barnett, V.A. Fassel, R.N. Kniseley, *Spectrochim. Acta* **28B**, 643 (1968)
- A.W. Miziolek, V. Palleschi, I. Schechter, *Laser-Induced Breakdown Spectroscopy (LIBS)—Fundamentals and Applications* (Cambridge University Press, New York, 2006)